

## Evolution of AQL X-1 During the Rising Phase of its 1998 Outburst

Wei Cui<sup>1</sup>, Didier Barret<sup>2</sup>, S. N. Zhang<sup>3,4</sup>, Wan Chen<sup>5,6</sup>, Laurence Boirin<sup>2</sup>, and Jean Swank<sup>5</sup>

### ABSTRACT

We present results from 16 snapshots of Aql X-1 with the *Rossi X-ray Timing Explorer* during the rising phase of its recent outburst. The observations were carried out at a typical rate of once or twice per day. The source shows interesting spectral evolution during this period. Phenomenologically, it bears remarkable similarities to “atoll” sources. Shortly after the onset of the outburst, the source is seen to be in an “island” state, but with little X-ray variability. It then appears to have made a rapid spectral transition (on a time scale less than half a day) to another “island” state, where it evolves slightly and stays for 4 days. In this state, the observed X-ray flux becomes increasingly variable as the source brightens. Quasi-period oscillation (QPO) in the X-ray intensity is detected in the frequency range 670–870 Hz. The QPO frequency increases with the X-ray flux while its fractional rms decreases. The QPO becomes undetectable following a transition to a “banana” state, where the source continues its evolution by moving up and down the “banana” branch in the color-color diagram as the flux (presumably, the mass accretion rate) fluctuates around the peak of the outburst. Throughout the entire period, the power density spectrum is dominated by very-low frequency noises. Little power can be seen above  $\sim 1$  Hz, which is different from typical “atoll” sources. In the “banana” state, the overall X-ray variability remains low (with fractional rms  $\sim 3$ –4%) but roughly constant. The observed X-ray spectrum is soft with few photons from above  $\sim 25$  keV, implying the thermal origin of the emission. The evolution of both spectral and temporal X-ray properties is discussed in the context of disk-instability models.

*Subject headings:* accretion, accretion disks – stars: individual (Aql X-1) – stars: neutron – X-rays: stars

---

<sup>1</sup>Room 37-571, Center for Space Research, Massachusetts Institute of Technology, Cambridge, MA 02139

<sup>2</sup>Centre d’Etude Spatiale des Rayonnements, 9 Av du Colonel Roche, 31028 Toulouse Cedex 04, FRANCE

<sup>3</sup>ES-84, NASA/Marshall Space Flight Center, Huntsville, AL 35812

<sup>4</sup>also Universities Space Research Association

<sup>5</sup>NASA/Goddard Space Flight Center, Code 661, Greenbelt, MD 20771

<sup>6</sup>also Department of Astronomy, University of Maryland, College Park, MD 20742

## 1. Introduction

Soft X-ray transients (SXTs) constitute an important subclass of low-mass X-ray binaries. For most of the time, they appear as extremely faint X-ray sources, if detected at all, but occasionally they brighten up by orders of magnitude in X-ray intensity, becoming the brightest X-ray sources in the sky in some cases. There appears to be some consensus that thermal instability causes a sudden surge in the mass accretion rate through the disk and, thus, initiates an X-ray outburst (review by King 1995 and references therein). Archival databases have been established over the years for the study of SXTs in outbursts and have been continually enriched by the on-going missions. Few observations, however, have been made of SXTs during the rising phase of an outburst because of the difficulty in catching such a brief period (typically lasting for a few days; cf., Chen, Shrader, & Livio 1997). The situation has greatly improved with the launch of *Rossi X-ray Timing Explorer* (RXTE; Bradt, Rothschild, & Swank 1993). *RXTE* carries an all-sky monitor (ASM) that continuously scans the sky for transient events. Upon detection, the main instruments can be re-programmed to observe the event within hours. To take advantage of these unprecedented capabilities, we have established a comprehensive program to sample the rising phase of an outburst at a high rate, in order to facilitate systematic studies of the phenomenon. Luckily, we have already caught several outbursts from different sources since the beginning of this year. In this Letter, we present results from observations of Aql X-1 during the rising phase of its recent outburst (Swank et al. 1998).

Aql X-1 belongs to a minority group of SXTs that have been determined to contain neutron stars (as opposed to black holes) because they display Type I X-ray bursts. It is known to experience frequent outbursts (roughly once every year; see, e.g., Friedhorsky & Terrell 1984; also public ASM/RXTE light curves). The *RXTE* observations of Aql X-1 during a previous outburst have revealed the presence of quasi-periodic oscillations (QPOs) near kHz range in the X-ray light curves (Zhang et al. 1997), which seem to be common for X-ray binaries with a weakly magnetized neutron star (review by van der Klis 1997). The kHz QPO phenomenon is currently thought to be associated with the accretion disk, perhaps representing processes varying on dynamical time scales in the inner portion of the disk. There is suggestive evidence that the magnetic field might play a crucial role in actually producing the observed X-ray modulation (see, e.g., Zhang, Yu, & Zhang 1998). One of the neutron star SXTs, 4U 1608-52, is further classified as an “atoll” source, whose neutron star is thought to have even weaker magnetic field than a “Z” source (van der Klis 1995). The classification of Aql X-1 in this scheme is not certain.

Near the end of February 1998, the ASM detected the onset of an outburst from Aql X-1 (Swank et al. 1998). Fig. 1 shows a portion of the long-term ASM light curve for the source that highlights the event. The outburst peaked at roughly 34 c/s (or  $\sim 450$  mCrab in the 1.3-12 keV band). The initial rise lasted for about 12 days. The pending Target-of-Opportunity proposals of ours were triggered by the ASM alert, subsequently, a series of pointed *RXTE* observations were carried out.

## 2. Observations

The data used for this study come from a total of 16 snapshots of Aql X-1 with the *Proportional Counter Array* aboard *RXTE*, covering a major portion of the rising phase and the peak of the outburst. The times when these observations were made are indicated in Fig. 1. The first observation took place when the ASM flux was about one quarter of the peak value. Each pointed *RXTE* observation lasted for one satellite orbit with an effective exposure time in the range 1.2–3.6 ks. The observations were conducted at a typical rate of once or twice per day, with occasional gaps due to scheduling constraints. Besides the two *Standard* data modes, a combination of *Burst Trigger* and *Burst Catcher* modes were used to zoom in onto any Type I bursts detected; but, no X-ray bursts were seen. An *Event* mode with  $\sim 122\mu\text{s}$  timing resolution and 64 energy bands was adopted to facilitate high-resolution timing analysis with a moderate energy resolution.

## 3. Data Analysis and Results

We have carried out preliminary spectral analysis, using the *Standard 2* data. Throughout the entire period, the observed X-ray spectrum can be modeled quite well by a composite of a blackbody (BB) component (for emission from the neutron star surface), a multi-color disk (MCD) component (for emission from the accretion disk), and a thermal bremsstrahlung component (for emission from hot plasma perhaps present in the vicinity of the neutron star); an emission line at  $\sim 6.6$  keV is also required. Fig. 2 shows the evolution of the BB and MCD components. The spectrum remains soft, with few photons above  $\sim 25$  keV, implying the thermal origin of the emission. The fluxes have been computed using the best-fit parameters, with the H I column density fixed at  $5 \times 10^{21} \text{ cm}^{-2}$  (Christian & Swank 1997) during the fit. The discussion of physical models for such a spectrum is beyond the scope of this work; it will be presented in a future paper on detailed spectral modeling.

For each observation, we have made light curves (with background subtracted) from the *Standard 2* data (with 16-second timing resolution) in three energy bands: 2–5.2 keV, 5.2–8.9 keV, and 8.9–19.7 keV, from which two hardness ratios, 5.2–8.9 keV/2–5.2 keV (soft color) and 8.9–19.7 keV/5.2–8.9 keV (hard color), have been calculated. The results are summarized in Fig. 3a, in the form of a color-color diagram for each observation. Fig. 3b shows the overall spectral evolution by putting together all the results. There are two apparent spectral transitions between three disjointed branches. Initially, the source is on the upper of the two left branches. It then seems to have made a rapid spectral transition to the lower one (on a time scale less than half a day; see Fig. 1). As the X-ray flux increases, the source evolves slightly, moving from the upper-right side to the lower-left side, and stays on this branch for 4 days before making another transition to the right branch. Subsequently, the source continues its evolution by moving up and down the branch from left to right as the source flux fluctuates around the peak of the outburst.

Using the *Event* mode data, we have carried out FFT for every 128-second data segment of each observation. Individual power-density spectra (PDSs) are then properly weighted and co-added to obtain the average PDS for the observation. A kHz QPO is detected only when the source is on the left lower branch of the color-color diagram (see Fig. 4 for an example). The QPO profile can be modeled well by a simple Lorentzian function, and the best-fit parameters are shown in Table 1. The errors are estimated based on  $\Delta\chi^2 = 1$ . From the table, we can see that the QPO frequency varies in the range 670–870 Hz and width (FWHM) in the range 9–20 Hz. As the flux increases, the QPO frequency also increases, and appears to have reached a plateau at  $\sim 850$  Hz (following Observation 3; see Table 1); the fractional rms decreases. We have also performed FFT for different energy bands to investigate the energy dependence of the QPO. The results show that the fractional rms increases almost linearly with energy, up to  $\sim 20\%$  in the 13.1–19.7 keV band. The QPO becomes unmeasurable following the second transition.

Except for the first observation, the power-density continuum is dominated by low-frequency “1/f” noises (with the power-law slope varying in the range -0.8– -1.5); very little power is measured above  $\sim 1$  Hz (see, e.g., Fig. 4). The source shows very little variability when it is on the left upper branch (i.e., Observation 1). It becomes more variable, following the first transition. The measured fractional rms (for the continuum) increases from  $\sim 1.5\%$  and to  $\sim 6.4\%$ . The variability seems to drop slightly, following the second transition to the right branch, with the fractional rms staying at  $\sim 3\text{--}4\%$  subsequently.

## 4. Discussion

### 4.1. Is Aql X-1 an “Atoll” Source?

The phenomenology of the observed spectral evolution is very similar to that of “atoll” sources (van der Klis 1995, and references therein). In the color-color diagram (Fig. 3b), the left branches may represent so-called “island” states, while the curved right branch certainly shows the characteristics of a “banana” state. As the observed X-ray flux (presumably, the mass accretion rate) increases, the source moves from one “island” to another, then to the “banana” branch. Fig. 3a shows that the correlation between spectral states and mass accretion rate holds remarkably well in detail. For instance, as soon as the X-ray flux begins to drop in observations 15 and 16, the source reverses its motion along the branch and moves from right to left down the “banana”. Perhaps, Aql X-1 should be classified as an “atoll” source, like its cousin 4U 1608-52. However, Aql X-1 also differs from 4U 1608-52 or other typical “atoll” sources in that the high-frequency noise component (van der Klis 1995) is absent from the measured PDS for both the “island” states and “banana” state.

For “atoll” sources, the physical processes that trigger the transition between “island” states themselves or between an “island” state and a “banana” state are still not well understood. In the following, we discuss a physical scenario that can account for the observed spectral and temporal

evolution of Aql X-1 during the rising phase of the outburst, based on our current knowledge of SXTs and their outburst mechanisms.

#### 4.2. Transition between “Island” States

It is thought that for SXTs in quiescence the mass accretion process is likely to operate in the form of “advection-dominated” accretion flows (ADAFs; Narayan & Yi 1994, 1995; Narayan 1997). In this regime, the compact object is surrounded by a hot ADAF region that is sub-Keplerian and experiences a phase transition to the standard thin disk (Shakura & Sunyaev 1973) thousands of Schwarzschild radii away (Narayan 1997). In the context of disk instability models, when thermal instability sets in, the mass accretion rate surges, thus, an outburst is under way. In the process, the ADAF region is cooled efficiently via inverse Compton scattering processes, because of the increase of “seed” photons from the disk. Consequently, the region shrinks; at the same time, the thin disk in the outer region fills in. Such a transition is likely to continue until the inner edge of the disk reaches the last (marginally) stable orbit (Narayan 1997). Although many details in the ADAF model, such as the location of the transition zone between the ADAF and the thin disk, still need to be worked out, the general evolution sequence has been shown to be followed well (see, e.g., Esin, McClintock, & Narayan 1997).

For SXTs that contain a neutron star, the effects of magnetic field must be taken into account. Unfortunately, neither do we know the precise configuration of the magnetic field in the presence of an accretion disk, nor do we fully understand the disk-field interaction (see, e.g., Ghosh & Lamb 1979 and Lovelace, Romanova, & Bisnovatyi-Kogan 1995). Assuming a simple dipole field, the magnetospheric radius is given by (see, e.g., Lamb, Pethick, & Pines 1973 and Cui 1997)

$$r_m = 10^7 \xi L_{x,36}^{-2/7} M_{1.4}^{1/7} B_9^{4/7} R_6^{10/7} \text{ cm} \quad (1)$$

where  $\xi$  is a model-dependent and dimensionless number, ranging from 0.52 (Ghosh & Lamb 1979) to  $\sim 1$  (Arons 1993; Ostriker & Shu 1995; Wang 1996);  $L_{x,36}$  is the bolometric X-ray luminosity in units of  $10^{36} \text{ ergs/s}$ ;  $B_9$  is the dipole field strength at the poles in units of  $10^9 \text{ G}$ ;  $M_{1.4}$  is the mass of the neutron star in units of  $1.4M_\odot$ , and  $R_6$  is its radius in units of 10 km.

At the beginning of an outburst, the mass accretion rate is low, so the magnetosphere initially extends much beyond the last stable orbit. As the inner edge of the disk subsequently moves in toward the neutron star, it is bound to encounter the magnetosphere first. We argue that it is the onset of this disk-field engagement that might have caused the transition between the two “island” states. Perhaps, observations 1 and 2 were made just before and after the engagement. For Observation 2,  $L_{x,36} = 5.7$  (for a source distance of 2.5 kpc, after being corrected for absorption), so  $r_m = 61\xi B_9^{4/7} \text{ km}$ . For  $r_m > 3R_s$  (the radius of the last stable orbit for a slowly rotating neutron star), where  $R_s$  is the Schwarzschild radius,  $B_9 > 0.062$  (or 0.20) for  $\xi = 1$  (or 0.52).

As the mass accretion rate increases, the BB temperatures increases, as shown in Fig. 2.

At the same time, the magnetosphere is pushed back further, so the disk extends closer to the neutron star and becomes hotter (also Fig. 2). The intensified emission, both from the neutron star surface and accretion disk (mostly in the 2–5.2 keV band, and also in the 5.2–8.9 keV band), results in the decrease of hardness ratios as the source evolves in the second “island” state.

### 4.3. Transition between “Island” and “Banana” States

The evolution continues until the mass accretion rate becomes so large that the magnetosphere is entirely inside the last stable orbit (as indicated by the constancy of the inferred radius of the inner edge of the disk following Observation 6; see Fig. 2). Then, the disk is once again disengaged from the magnetic field. This might have triggered the transition from the lower “island” state to the “banana” state, as indicated by the disappearance of the kHz QPO. Then, an *upper* limit could be derived for the magnetic field from equation (1). The transition is clearly under way during Observation 6. For this observation,  $L_{x,36} = 10.7$ , so  $r_m \lesssim 3R_s$  leads to  $B_9 \lesssim 0.085$  (or 0.27) for  $\xi = 1$  (or 0.52).

In the “banana” state, the observed spectral evolution implies that the soft fluxes (both from the disk and the neutron star surface) shift more toward the the middle energy band (5.2-8.9 keV), as the mass accretion rate increases, and the hard flux increases even more.

### 4.4. Summary

We have proposed a simple explanation for the observed spectral and temporal evolution of Aql X-1 during the rising phase of the outburst. It remains to be seen whether or not the model also applies to “atoll” sources in general. Progress can be made by carefully studying “atoll” sources in a similar way (i.e., correlating the occurrence of kHz QPOs with distinct spectral states). The model is almost certainly over-simplified, but seems to be qualitatively valid.

It has been speculated that kHz QPOs might originate in the inhomogeneity (or “hot spots”) at the inner edge of the disk and the QPO frequency might simply be the local Keplerian frequency or the beat frequency between the Keplerian motion and the spin of the neutron star (see van der Klis 1997 for a review). If so, the occurrence and disappearance of the kHz QPO for Aql X-1 would strongly suggest that the magnetic field plays an essential role in producing such “hot spots” by interacting with the disk. With limited statistics (Table 1), the kHz QPO frequency does seem to level off as the mass accretion rate continues to increase, perhaps indicating that the inner edge of the disk has reached (or approached close to) the last stable orbit as early as Observation 3. This is not inconsistent with the spectral results (see Fig. 2).

It is instructive to compare this outburst with previous ones. A spectral transition was also observed near the end of the decaying phase of the first 1997 outburst (Zhang, Yu, & Zhang 1998).

It appears to be similar to the first transition observed here, although it started at a lower flux level. Interestingly enough, the kHz QPO was also detected at lower fluxes (Zhang et al. 1998). Although it is true that the peak intensity of the current outburst is higher than the previous one, it is not clear how this would affect the fundamental properties of the system. It is possible, however, that the disk structure might be different between the rising and decaying phases, which could result in hysteresis. More studies are clearly required to address this issue.

This work is supported partially by NASA through Contract NAS5-30612. We would like to thank Alan Harmon and Jean Francois Olive for helpful discussions.

## REFERENCES

- Arons, J. 1993, *ApJ*, 408, 160
- Bradt, H. V., Rothschild, R. E., & Swank, J. H. 1993, *A&AS*, 97, 355
- Chen, W., Shrader, C. R., & Livio, M. 1997, *ApJ*, 491, 312
- Christian, D. J., & Swank, J. H. 1997, *ApJS*, 109, 177
- Cui, W. 1997, *ApJ*, 482, L163
- Esin, A. A., McClintock, J. E., & Narayan, R. 1997, *ApJ*, 489, 865
- Ghosh, P., & Lamb, F. K. 1979, *ApJ*, 234, 296
- King, A. R. 1995, in “X-ray Binaries”, eds. W. H. G. Lewin, J. van Paradijs, & E. P. J. van den Heuvel (Cambridge U. Press, Cambridge) p. 419
- Lamb, F. K., Pethick, C. J., and Pines, D. 1973, *ApJ*, 184, 271
- Lovelace, R. V. E., Romanova, M. M., & Bisnovatyi-Kogan, G. S. 1995, *MNRAS*, 275, 244
- Narayan, R., & Yi, I. 1994, *ApJ*, 428, L13
- Narayan, R., & Yi, I. 1995, *ApJ*, 444, 231
- Narayan, R. 1997, in “Accretion Phenomena and Related Outflows”, eds D. T. Wickramasinghe, G. V. Bicknell, & L. Ferrario, *ASP Conf. Series Vol. 121*
- Ostriker, J., & Shu, F. 1995, *ApJ*, 477, 813
- Priedhorsky, W. C., & Terrell, J. 1984, *ApJ*, 280, 661
- Shakura, N. I., & Sunyaev, R. A. 1973, *A&A*, 24, 337
- Swank, J. H., Smith, E., Levine, A. M., & Remillard, R. 1998, *IAU Circ.* 6828
- van der Klis, M. 1995, in “X-ray Binaries”, eds. W. H. G. Lewin, J. van Paradijs, & E. P. J. van den Heuvel (Cambridge U. Press, Cambridge) p. 252
- van der Klis, M. 1997, to appear in *Proc. NATO Advanced Institute “The Many Faces of Neutron Stars,”* Lipari, Italy, 1996
- Wang, Y.-M. 1996, *ApJ*, 465, L111
- Zhang, S. N. Yu, W. & Zhang, W. 1998, *ApJ*, 494, L71
- Zhang, W., Jahoda, K., Kelley, R. L., Strohmayer, T. E., Swank, J. H., & Zhang, S. N. 1998, *ApJ*, 495, L9



Table 1. Observed kHz QPO in Aql X-1

Observation	Frequency (Hz)	FWHM (Hz)	Fractional RMS (%)
2	$677.0^{+0.4}_{-0.3}$	$9.1^{+0.7}_{-0.9}$	$6.3^{+0.2}_{-0.2}$
3	$856.3^{+1.1}_{-1.0}$	$19.7^{+2.5}_{-2.0}$	$5.7^{+0.3}_{-0.2}$
4	$839.5^{+0.5}_{-0.4}$	$11.0^{+1.1}_{-0.9}$	$5.7^{+0.2}_{-0.2}$
5	$871.4^{+1.0}_{-1.0}$	$11.8^{+3.0}_{-2.4}$	$3.3^{+0.3}_{-0.3}$

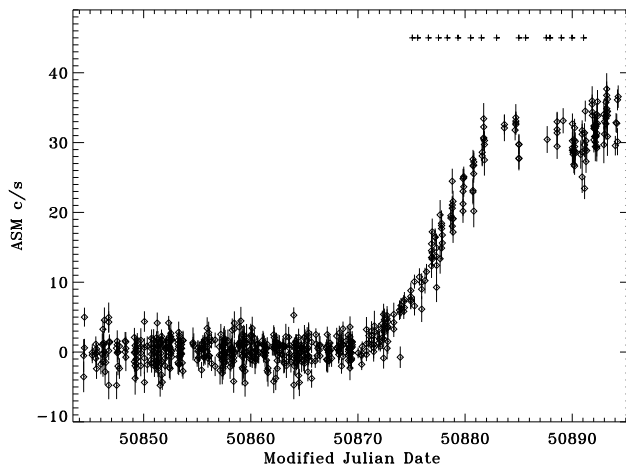


Fig. 1.— ASM light curve for Aql X-1. Each data point represents a 90-second measurement. Note that the outburst started roughly at MJD 50870 (2/26/98). As a reference, the Crab Nebula produces about 75 c/s. The crosses indicate the times when the pointed *RXTE* observations were carried out. The pointed observations are numbered sequentially, starting from Observation 1, throughout the text.

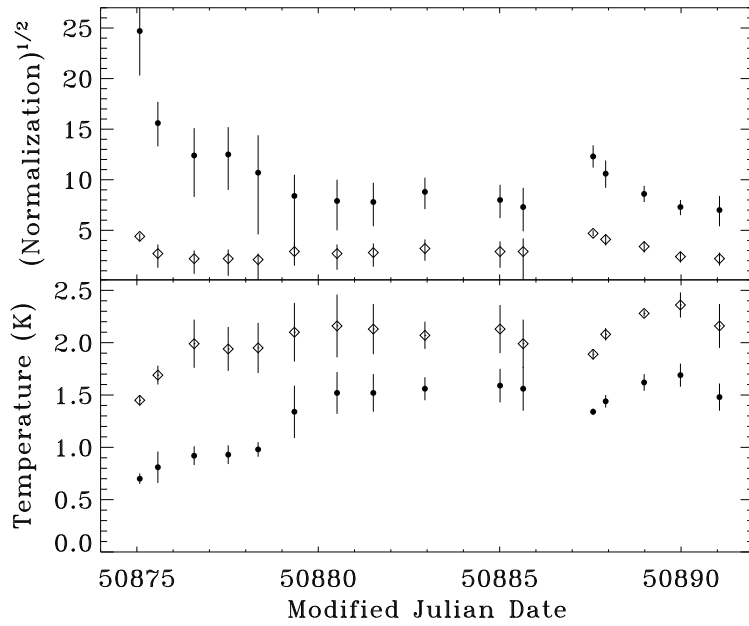


Fig. 2.— Evolution of the BB (diamonds) and MCD (bullets) components. For MCD, the temperature shown is for the inner edge of the accretion disk. Note that the upper panel essentially shows  $R_{BB}/D$  and  $R_{in}(\cos i)^{1/2}/D$  for BB and MCD, respectively, where  $R_{BB}$  is the radius of the BB emission region in units of km;  $R_{in}$  is the radial distance to the inner edge of the disk in units of km;  $i$  is the inclination angle of the disk; and  $D$  is the distance to the source in units of 10 kpc.

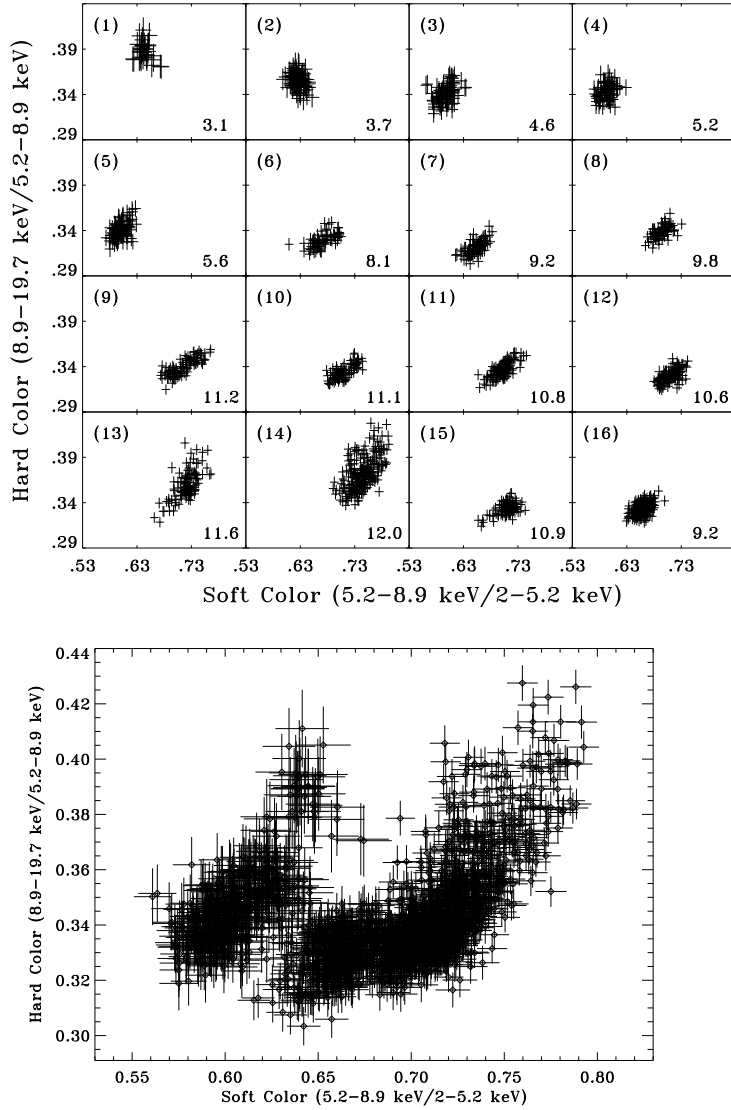


Fig. 3.— (a) Color-color diagram for each observation. Each data point represents a 16-second measurement. The measured 2–25 keV fluxes in units of  $10^{-9} \text{ ergs cm}^{-2} \text{ s}^{-1}$  are also shown at the lower right-hand corner of each panel. Note that the source moves up and down the right branch of the overall color-color diagram (bottom panel) as the X-ray flux fluctuates around the peak of the outburst. (b) Overall color-color diagram. Note the transitions between three distinct branches. The kHz QPO is only detected when the source is on the left lower branch.

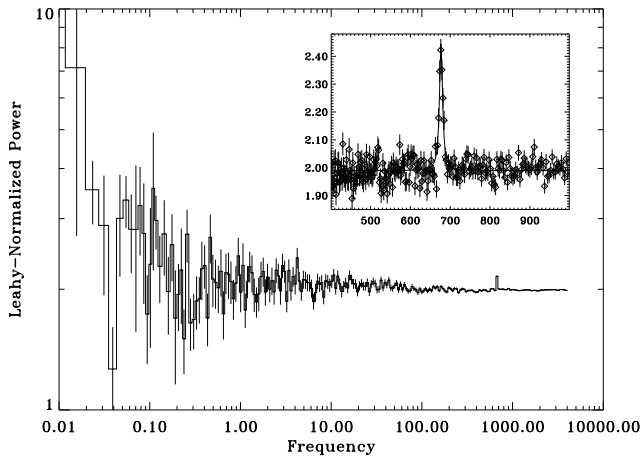


Fig. 4.— A sample power-density spectrum (taken from Observation 2). Note the presence of very low-frequency noises and a kHz QPO. The inset shows the QPO profile in detail, with the solid line representing the best-fit Lorentzian function.